Wood Science and Technology 32 (1998) 335–345 © Springer-Verlag 1998

Spiral angle of elementary cellulose fibrils in cell walls of *Picea abies* determined by small-angle X-ray scattering

A. Reiterer, H. F. Jakob, S. E. Stanzl-Tschegg, P. Fratzl

Summary The spiral angle of the elementary cellulose fibril in the wood cell wall, often called microfibril angle, is of primary importance for the mechanical properties of wood. While there are a number of methods to estimate this angle, x-ray diffraction (XRD) techniques have recently obtained a lot of attention because of their ability to provide information averaged over a significantly large specimen volume. Here, we present results from a related method, small-angle x-ray scattering (SAXS). The advantage of SAXS is that, unlike XRD, it does not require any assumption on the orientation of the cellulose crystal axis with respect to the fibril axis. Full three-dimensional scattering patterns were collected using an area detector by rotating the sample around one axis. The distribution of fibrillar orientations was seen to reflect the typical cross-sectional shape of the tracheids (square or circular). In the stem, the spiral angle was found $<5°$ in earlywood and $\approx 20°$ in latewood. In branches the angle was $\approx 30°$ in the upper part and $\approx 40°$ in the lower part, which strongly supports the idea that the spiral angle has primarily mechanical function.

Introduction

The determination of spiral angles is currently attracting an increased interest (Sahlberg et al. 1997, Cave 1997a, b), as they are considered to influence the mechanical properties of wood (Cave and Walker 1994).

Received 12 June 1997

A. Reiterer, S. E. Stanzl-Tschegg
Institut für Meteorologie und Physik der Universität
für Bodenkultur Wien, Türkenschanzstr. 18, A-1180 Wien, Austria

H. F. Jakob
Institut für Materialphysik der Universität Wien,
Strudlhofgasse 4, A-1090 Wien, Austria

Correspondence to: P. Fratzl
Erich-Schmidinstitut der ÖAW &
Univ. Leoben, Jahnstr. 12, A-8700 Leoben
Austria
e-mail: fratzl@unileoben.ac.at

We thank W. Laube, F. Einramhof, H. Königshofer and H. Löppert for their technical assistance. Financial support from the Fonds zu Förderung der Wissenschaftlichen Forschung (Proj. P10729-BIO) is gratefully acknowledged

According to the current cell wall models of spruce wood (Fengel and Wegener 1984, Sell and Zimmermann 1997), which consists to 95% of tracheids, the major part of the cell wall – labeled S_2 – contains a system of very long but thin parallel cellulose fibrils embedded in a matrix of hemicellulose and lignin. This S_2 makes up between 79 and 86% of the cell wall (Fengel and Stoll 1973). The orientation of the fibrils is given by a spiral angle α with respect to the longitudinal direction of the tracheid (i.e., of the stem or of the branch). In the second largest layer of the cell wall – labeled S_1 – the fibrils run at a gentle helical slope roughly perpendicular to the ones in the S_2 (Fengel and Wegener, 1984). All other components of the cell wall are much smaller.

The spiral angle in the S_2 (as in the other different cell wall layers) has been measured for various species (conifer and deciduous trees) using polarized light microscopy (PLM), staining methods (SM), x-ray-diffraction (XRD) as well as small-angle x-ray scattering (SAXS). A collection of data is given in Table 1. These data demonstrate, that the spiral angles vary considerably.

The staining methods for microscopic investigations require tedious sample preparation procedures (Robinson et al. 1987), which involve the danger of altering the structure of the sample. Obtaining good statistics is another difficulty of SM and PLM, as a great number of pictures have to be evaluated.

Sample preparation can be almost completely avoided by using one of the two scattering methods, XRD or SAXS, where native samples can be investigated. Both scattering methods average over the structures inside a macroscopic volume and good statistics are automatically obtained there. The XRD-technique has recently been described in detail (Cave 1997a, b). It is based on an evaluation of the angular distribution of the scattering intensity from a given crystallographic reflection. Typically, one assumes that there is no preferred orientation of the cellulose crystal axes around the microfibril axis which also means that there is no well defined orientation relation between the crystallographic planes and the cell wall. The SAXS-technique (Jakob et al. 1994, Fratzl et al. 1997) avoids this assumption by being sensitive to the density contrast between cellulose and the surrounding lignin/hemicelllulose matrix. Moreover, the use of an area detector allows the measurements of complete three-dimensional small-angle scattering patterns with rotation of the specimen around just one axis.

We present SAXS-results for the distribution of spiral angles in wood from *Picea abies*. In particular, we show the effects of a square cross-section of wood cells as well as differences in branches and in the stem.

Materials and methods

Specimen preparation

We selected normal, air-dried samples of spruce-wood, either from the stem or from the upper, respectively lower side of a branch. Tangential slices were cut out of these samples along the longitudinal direction of the branch within earlywood and latewood of the first three annual rings of the upper and the lower side and within latewood of the 7th and 18th annual ring of the upper side and of the 10th and 18th annual ring of the lower side of the branch. Slices were also cut within the latewood of the 50th annual ring of a stem which was free of reaction wood. The slices were investigated without further chemical or physical treatment. All specimens had the same thickness of 200 μm which turned out to be an optimum for SAXS (Jakob et al. 1994). They were encapsulated in a plastic foil of 50 μm thickness in order to prevent drying in the high vacuum of the x-ray apparatus.

Table 1. Summary of the fibrillar angle measured in various species. The table is not meant to be exhaustive

Authors	Method	Species	fibrillar angle [°]
Preston 1934	PLM	Cedar (branch)	39–57
		Japanese larch	37–79
		Abies nobilis	23–69
Kantola and Seitsonen 1961	XRD	*Pinus silvestris*	11 (normal wood) 35 (compression wood)
		Picea excelsa	32–35 (normal wood) 39–43 (compression wood)
		Juniperus communis	37 (normal wood) 40 (compression wood)
Kantola and Kähkönen 1963	SAXS	*Pinus silvestris*	small (normal wood) 33–40 (compression wood)
		Picea excelsa	18 (normal wood) 25–45 (compression wood)
		Juniperus communis	40–43 (compression wood)
		Betula pubescens	16 (normal wood) small (tension wood)
		Alnus incana	22 (normal)
Hiller 1964	SM	Loblolly pine	4–25 (latewood)
		Slash pine	10–40 (latewood)
Mark 1967	PLM	Virginia Pine	20
Kantola and Seitsonen 1969	XRD SAXS	*Picea excelsa*	4–54
El-Osta et al. 1972	XRD	Douglas fir	20 (early- and normal wood)
	SM		28 (early- and compression wood) 13 (late- and normal wood)
		Sitka spruce	17 (late- and compression wood) 13 (earlywood)
		Western hemlock	17 (latewood) 22 (earlywood) 21 (latewood)
El-Osta et al. 1973	XRD	Douglas fir	15–27 (earlywood) 11–18 (latewood)
		Western hemlock	8–9 (earlywood)
Tang 1973	PLM	Virginia pine	24 (earlywood) 17 (latewood)
Erickson et al. 1974	PLM	Douglas fir	7–30
Boyd and Foster 1974	PLM	*Pinus radiata*	12–27
Paakkari and Serimaa 1984	XRD	Pine, spruce	5 (normalwood) 22 (compression wood)
Jakob et al. 1994	SAXS	*Picea abies*	<5 (earlywood) 20 (latewood)
Sahlberg et al. 1997	XRD	*Picea abies*	8 (earlywood) 9 (Latewood)

The longitudinal direction of the samples (i.e. the direction of the branch axis) was perpendicular to the incoming x-ray beam.

SAXS-Measurements

The scattering intensity $I(\vec{q})$ was recorded as a function of the scattering vector $\vec{q}$ with modulus $q = |\vec{q}| = \frac{4\pi}{\lambda}\sin(\theta)$, where 2θ is the angle between the incoming and the scattered x-ray beam. Scattering patterns were recorded with a typical time of half an hour per spectrum to provide sufficient counting statistics. The scattering intensity $I(\vec{q})$ was corrected for the occuring background scattering from the encapsulating foil.

The experimental setup consisted of a 12 kW rotating anode x-ray generator used in a point-focus geometry. The incoming x-ray beam had a circular cross section of 0.6 mm in diameter. The radiation wavelength was $\lambda = 0.154$ nm, corresponding to Cu-K_α radiation in combination with a Ni-filter. The spectra were taken with a two-dimensional position sensitive detector (Fa. AXS) with a sample to detector distance of 98.5 cm.

Determination of spiral angle

The evaluation of SAXS-patterns from wood has been described in detail earlier (Jakob et al. 1994 and 1995). Since the main goal in this study was the determination of the spiral angle, it is sufficient to realize that the SAXS-signal from a long rod (the elementary cellulose fibril) has the shape of a flat disk perpendicular to the fibril. Hence, any measurement with an area detector will produce a section across this disk, which will be seen as a streak in the plane of observation. Several such streaks are shown in Fig. 1c, d and g.

Using similar notations as Cave 1997, we call μ the angle between the axis of the tracheid and of the elementary cellulose fibril. The angle between the plane of observation (containing the tracheid axis) and the plane defined by the tracheid axis and the cellulose fibril is called β. The angle in the plane of observation (the area detector) where streaks are formed is called ψ_s (see Fig. 1c, d, g).

With these definitions it follows that

$$\mathrm{tg}\psi_s = \mathrm{tg}\mu\,\cos\beta \qquad (1)$$

(Kantola and Kähkönen 1963). Hence, if $\beta = 0°$ (that is, when the cell-wall is parallel to the plane of the detector) the direction of the streak indicates directly the spiral angle ($\mu = \psi_s$, see Fig. 2). If $\beta \neq 0°$, ψ_s is smaller than μ and can even be zero when the cell-wall is perpendicular to the area detector. Similar relations also occur in XRD measurements (see e.g. equation (4) in Cave 1997). In the special case of a square shaped cross-section of the tracheids, cell walls appear simultaneously with the orientations β, $\beta + 90°$, $\beta + 180°$ and $\beta + 270°$. Consequently, four streaks are generally expected at the angles ψ_s given by

$$\mathrm{tg}\psi_s = \pm\mathrm{tg}\mu\,\cos\beta \quad \text{and} \quad \mathrm{tg}\psi_s = \pm\mathrm{tg}\mu\,\sin\beta\ . \qquad (2)$$

If $\beta = 0°$, two of the streaks coincide, so that only three remain separated, located at $\psi_s = \pm\mu$ and at $\psi_s = 0°$ (see Fig. 3a, b). This is the most interesting geometry since μ can be read directly from the original data, such as in Fig. 1g. If the tracheids have a circular cross-section, ψ_s will be obviously independent of β and the contribution of all elementary fibrils of a whole tracheid adds up to a distri-

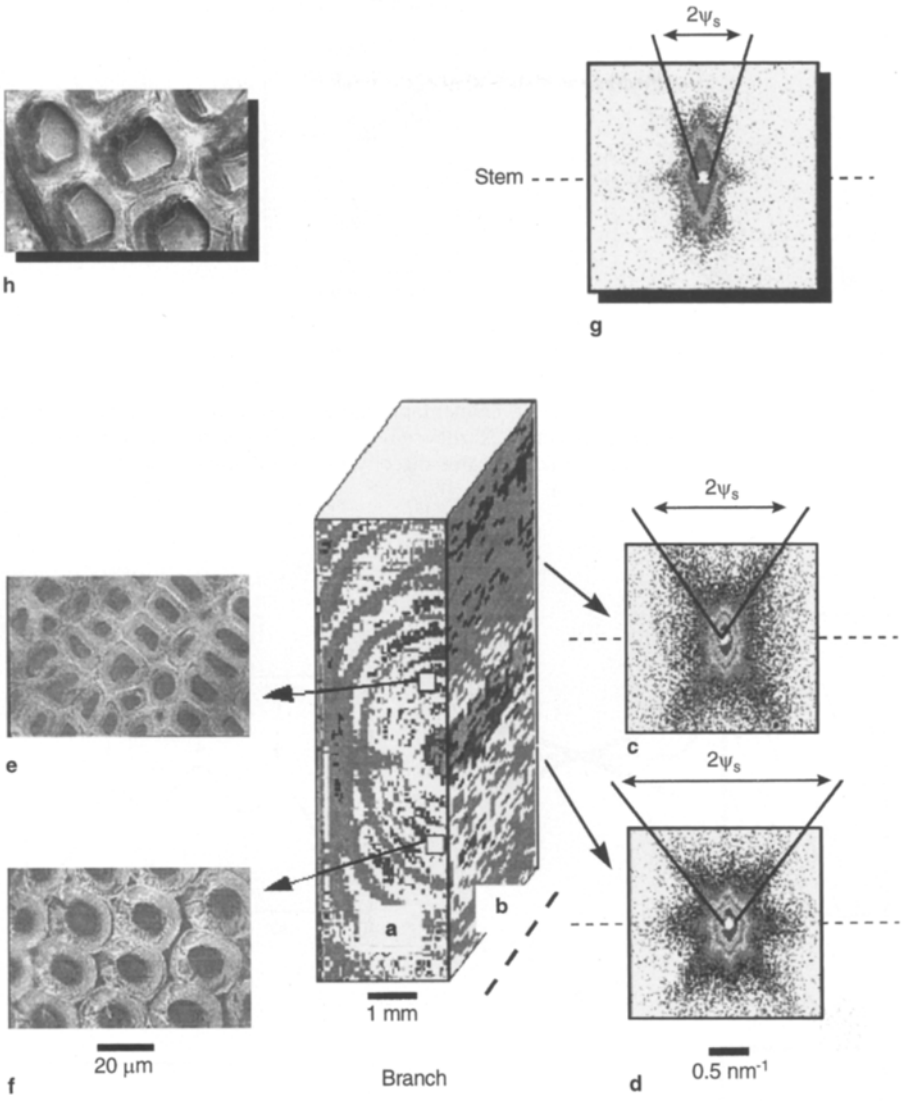

Fig. 1. Microradiography of (a) a cross-section and (b) a radial section of a branch of a spruce tree. The dotted line indicates the fibre direction (that is, the axis of the tracheids). Right, SAXS-pattern of a region typically under tension (c) and under compression (d). Left, light microscopic images of cross-sections showing the shape of the tracheids under tension (e) and under compression (f). For comparison a SAXS-pattern (g) and a light microscopic image (h) of latewood of a stem is also shown. The spiral angle ψ_s in the latewood of the lower side of the branch is higher than in the upper side of the branch and in the latewood of the stem

bution over ψ_s, strongly peaked at $\psi_s = \mu$ (see Fig. 2 in Kantola and Kähkönen 1963).

To estimate μ, two-dimensional SAXS-spectra (such as in Fig. 1c, d, g) were collected for a number of rotation angles β of the wood specimen around the longitudinal direction. For each data set, the total scattering intensity on the detector was plotted as a function of the polar angle ψ (see Fig. 4) and the maxima

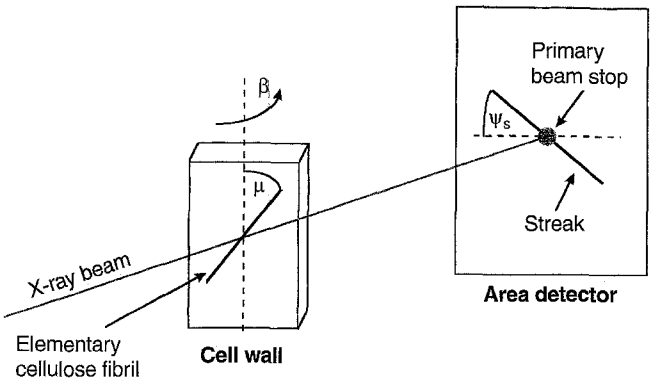

Fig. 2. Scattering geometry showing an elementary cellulose fibril in the cell wall and the streak produced on the area detector. If the cell wall is parallel to the area detector ($\beta = 0°$), the direction of the streak indicates directly the spiral angle ($\mu = \psi_s$)

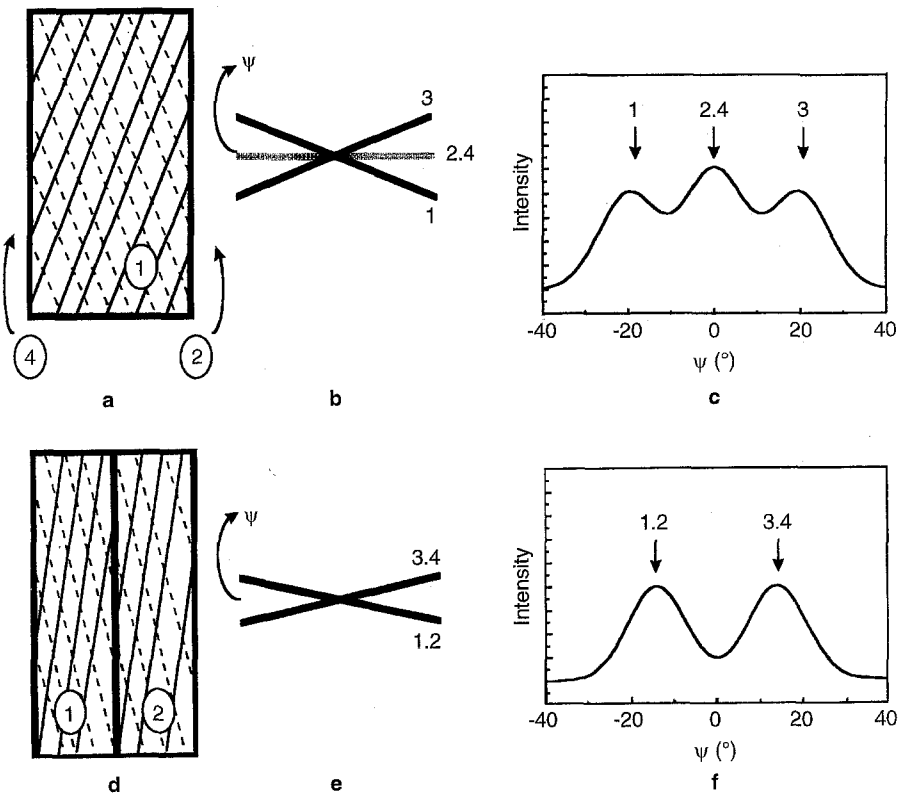

Fig. 3. Rotation dependence of the measured fibrillar angle for tracheids with rectangular cross-section. Four streaks are expected (equation 2). Two streaks, originating from elementary cellulose fibrils in walls 2 and 4, superimpose for a rotation angle $\beta = 0°$ (a, b) and $I(\psi)$ shows three maxima (c). For $\beta = 45°$, two streaks and two maxima can be detected (d, e and f)

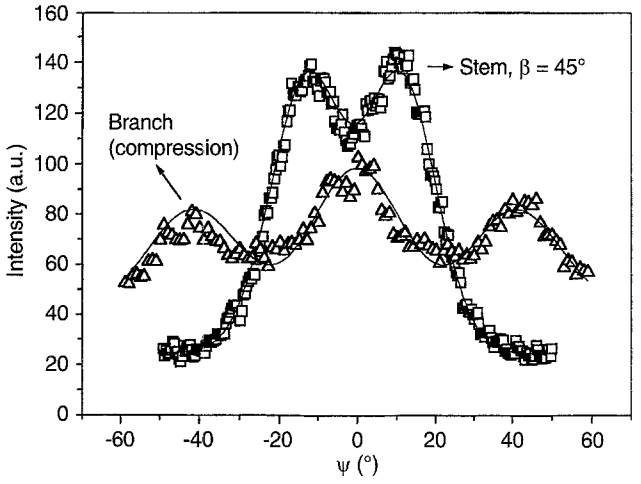

Fig. 4. Intensity distribution as obtained by ψ-integration of SAXS patterns of a stem (squares, rotation angle $\beta \approx 45°$) and of the upper part of a branch (triangles). The curves represent least-squares fits of the data using Gaussian-functions and assuming a constant background

were interpreted as streak directions and plotted as a function of β (see Fig. 5) to estimate the spiral angle μ.

Results

Two-dimensional SAXS-patterns were obtained for a number of specimens taken from different positions inside a branch from spruce-wood and integrated to obtain the intensity I(ψ) as a function of the polar angle ψ on the detector. For comparison, we also performed measurements with a specimen from latewood of the stem, where the spiral angle had been determined with the same method previously (Jakob et al. 1994).

The intensity distributions I(ψ) were fitted using Gaussian functions. An example is shown in Fig. 4 for a specimen from the lower side of the branch and another from latewood of the stem (rotation angle $\beta \approx 45°$). The maxima of these (up to four) Gaussian functions were then plotted as a function of β in graphs such as Fig. 5.

Spiral angle of latewood of a stem

In the graphs I(ψ), we typically found two to four maxima depending on the rotation angle β, which corresponds to the case of tracheids with rectangular cross-section (see Fig. 3).

The positions of the maxima of I(ψ), ψ_s, were plotted in Fig. 5a as a function of β. It shows that there were three maxima at $\beta = 0°$ (case shown in Fig. 3c), two at $\beta = 45°$ (case shown in Fig. 3f) and four at all other angles. The β-dependence visible in Fig. 5a may be quantitatively modeled by equation (2) where μ was assumed to be 18,8° (full lines in Fig. 5a). This is a strong confirmation of our earlier findings stating that the spiral angle is ≈20° in latewood of picea abies but it also shows that it is dangerous to interprete ψ_s if the orientation of the cell-wall with respect to the plane of orientation (that is, β) is unknown.

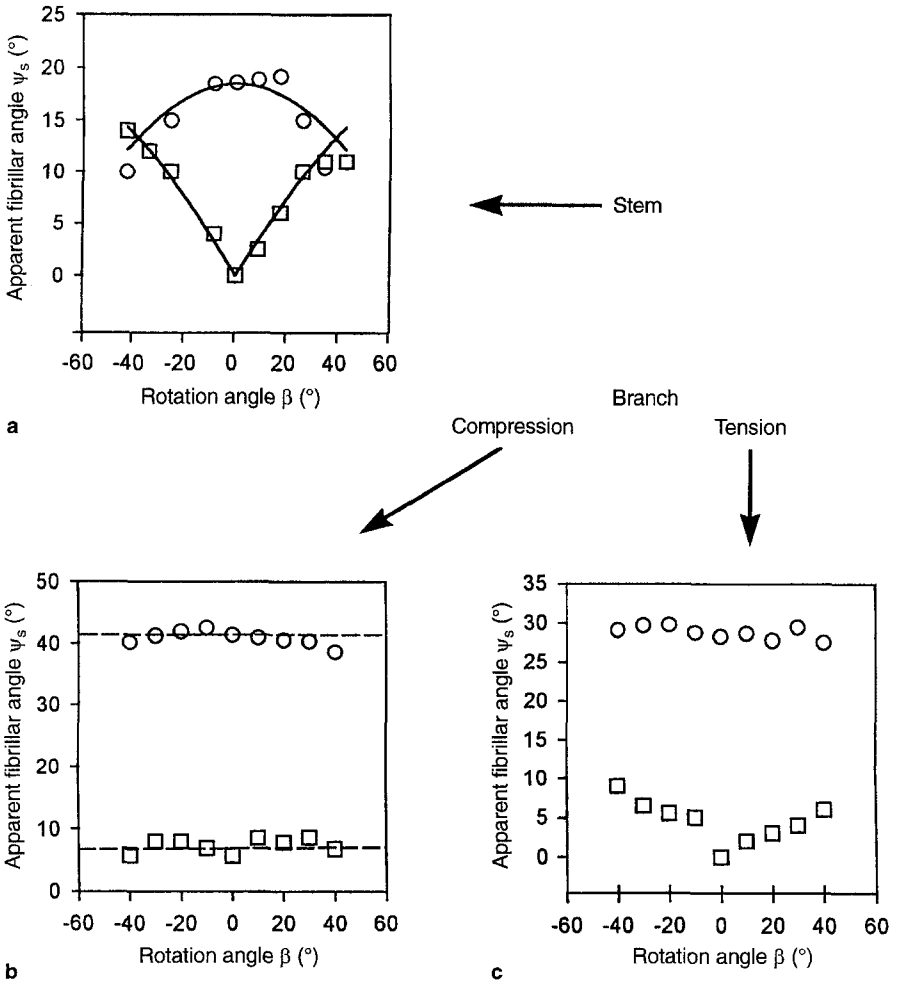

Fig. 5. Rotation dependence of the measured fibrillar angles for the latewood of a stem (a). The fibrillar angles for latewood of the lower side of the branch (b) show no rotation dependence. For the latewood of the upper side of the branch (c) the situation is somehow in-between. All plots are symmetrical around the horizontal axis ($I(\psi_s) = I(-\psi_s)$)

Spiral angle of the upper side of a branch

The cross-sections of the upper side of the branch show various forms (for example circular, rectangular and ellipsoid, see Fig. 1e). This fact has been reported by other authors (for example Core et al. 1979). The measured spiral angle has a certain rotation dependence (see Fig. 5c) but this dependence is caused by a mixture of the different shapes and cannot be represented by equation (2), however, the largest measured angle should always be the true fibrillar angle. Hence, μ was found to be $\approx 30°$ in the first three annual rings and also in the 7th and 18th annual ring. This situation is shown in Fig. 6. A second angle close to 5° is also seen. The relative amounts contributing to the total intensity are ≈50%. There was no difference between earlywood and latewood in this respect.

In the pith the fibrils were aligned with the direction of the wood cells, the spiral angle is <5°.

Spiral angle of the lower side of the branch

The cross-sections of tracheids of the lower side of the branch were circular. This is a well-known fact for reaction wood of conifers (Core et al. 1979, Lee and Eom 1988, Coté 1968). As a consequence, there was no rotation dependence of the measured spiral angle (Fig. 5b). The spiral angle was found to be ≈32° in the first two annual rings and increased to ≈40° in the third annual ring and to ≈42° in the 10th and 18th annual ring (Fig. 6). A second angle <5° could also be seen in all annual rings. The relative amounts contributing to the total intensity were ≈50%. Differences between earlywood and latewood could not be detected in these parameters.

Discussion

Small-angle x-ray scattering has been used to determine the spiral angle in different annual rings of a branch of spruce wood. As a first result, we found two well-separated angles, one smaller than 5° (that is, fibrils nearly parallel to the fibre direction in the branch) and a second one, much larger, varying between 30° and 40°. A comparison with the stem showed that the spiral angles are generally larger in the branch, both on the upper and on the lower side. Indeed, latewood of the stem contains tracheids with a spiral angle of ≈20° while the angle is <5° in earlywood (Jakob et al. 1994).

Such a clear separation between two types of cells could not be observed in the branch, where both early- and latewood featured a large spiral angle and one smaller than 5°. The data indicate that about half the elementary cellulose fibrils are in eitherone of the two configurations. This makes it very likely that both contributions come from the S2 cell-wall layer since the other parts of the cell wall are summing up to only ≈14–20% (Fengel and Wegener 1984).

It is not possible, however, to decide from the present data whether each cell wall in the branch contains sublayers with these two spiral angles or whether there is a mixture of tracheids with cell walls containing fibrils with just one of these two angles.

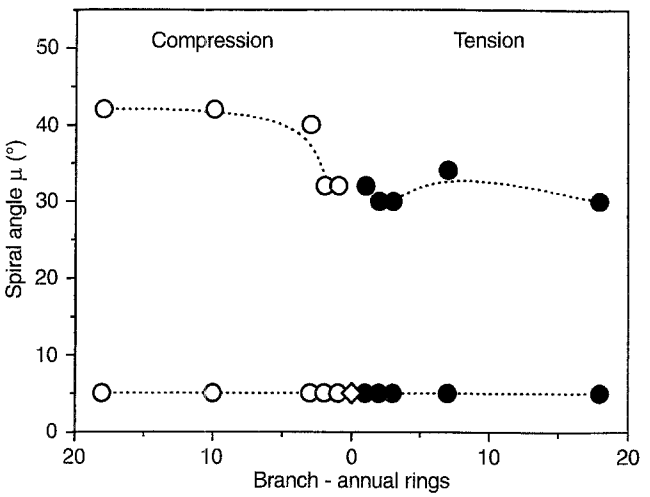

Fig. 6. Spiral angles in a branch of spruce wood. The solid symbols show the spiral angles in the upper part, the open symbols the spiral angles in the lower part. The diamond shows the spiral angle in the pith. The dotted lines are guides to the eye

From a mechanical point of view, it is interesting to note that the spiral angles are larger in the branch where much larger strains are to be expected owing to the movement in the winds and from gravitational forces. Apparently, the spiral angle is even larger on the lower side of the branch where compression forces will usually dominate. These observations are suggestive with respect to a mechanical function (Cave and Walker 1994) of the spiral angle.

Conclusion

The method of small-angle x-ray scattering, which is sensitive to the density contrast between cellulose and the lignin/hemicellulose matrix and not to the orientation of the cellulose crystal axes like the method of x-ray diffraction, was used to determine the spiral angles of spruce wood from a branch and of a stem. The spiral angles depended strongly on position and, hence, on sign and magnitude of the acting stress and strain. By collecting full three-dimensional SAXS-patterns the effects of different cross-sections of the tracheids on the SAXS signal could be shown.

References

Boyd JD (1977) Interpretation of X-Ray Diffractogramms of Wood for Assessments of Microfibril Angles in Fibre Cell Walls. Wood Sci. Technol. 11: 93–114

Boyd JD (1973) Appraising Methods of Measuring Microfibril Angles. Wood Science 6(1): 95–96

Boyd JD, Foster RC (1974) Tracheid Anatomy Changes as Response to Changing Structural Requirements of the Tree. Wood Sci. Technology 8: 91–105

Cave ID, Walker JCF (1994) Stiffness of wood in fast-grown plantation softwoods: the influence of microfibril angle. For. Prod. J. 44(5): 43–48

Cave ID (1997a) Theory of X-ray measurement of microfibril angle in wood, Part 1. The condition for reflection. Wood Sci. Technol. 31: 143–152

Cave ID (1997b) Theory of X-ray measurement of microfibril angle in wood, Part 2. The diffraction diagramm. Wood Sci. Technol. 31: 225–234

Core HA, Côté WA, Day AC (1979) Wood Structure and Identification. Second Edition, Syracuse University Press

Côté WA, Day AC, Timell TE (1968) Distribution of Lignin in Normal and Compression Wood of Tamarack. Wood Sci. Technol. 2:13–37

Cousins WJ (1972) Measurements of Mean Microfibril Angles of Wood Tracheids. Wood Sci.Technol. 6: 58

El-Osta MLM (1973) A Direct X-Ray Technique for Measuring Microfibril Angle. Wood and Fiber 5(2): 118–129

El-Osta MLM, Wellwood RW, Butters RG (1972) An Improved X-Ray Technique for Measuring Microfibril Angle of Coniferous Wood. Wood Science 5(2): 113–117

Fengel D, Stoll M (1973) Über die Veränderungen des Zellquerschnittes, der Dicke der Zellwand und der Wandschichten von Fichtentracheiden innerhalb eines Jahrringes. Holzforschung 27: 1–7

Fengel D, Wegener G (1984) Wood Chemistry, Ultrastructure, Reactions. De Gruyter, Berlin New York

Fratzl P, Jakob HF, Rinnerthaler S, Roschger P, Klaushofer K (1997) Position-resolved small-angle scattering of complex biological materials. J. Appl. Cryst. 30: 765–769

Hiller CH (1964) Correlation of Fibril Angle with Wall Thickness of Tracheids in Summerwood of Slash und Loblolly Pine. Tappi 47(2): 125–128

Jakob HF, Fengel D, Tschegg SE, Fratzl P (1995) The Elementary Cellulose Fibril in *Picea abies*: Comparison of Transmission Electron Microscopy, Small-Angle X-ray, and Wide-Angle X-ray Scattering Results. Macromolecules 26: 8782–8787

Jakob HF, Fratzl P, Tschegg SE (1994) Size and Arrangement of Elementary Cellulose Fibrils in Wood Cells: A Small-Angle X-Ray Scattering Study of *Picea abies*. J. Structural Biology 113: 13–22

Kantola M, Kähkönen H (1963) Small-Angle X-Ray Investigation Of The Orientation Of Crystallites in Finnish Coniferous and Deciduous Wood Fibers. Ann. Acad. Scient. Fenn. A VI 137
Kantola M, Seitsonen S (1961) X-Ray Orientation Investigations on Finnish Conifers. Ann. Acad. Scient. Fenn. A VI 80
Kantola M, Seitsonen S (1969) On the relation between Tracheid Length and Microfibrillar Orientation measured by X-Ray Diffraction in Conifer Wood. Ann. Acad. Scient. Fenn. A VI 300
Lee PW, Eom YG (1988) Anatomical Comparison between Compression Wood and Opposite Wood in a Branch of Korean Pine. IAWA Bulletin 12: 187–194
Meylan BA (1972) The Influence of Microfibril Angle on the Longitudinal Shrinkage-Moisture Content Relationship. Wood Sci. Technol. 6: 293–301
Meylan BA, Butterfield BG (1978) Helical Orientation of the Microfibrils in Tracheids, Fibres and Vessels. Wood Sci. Technol. 12: 219–222
Paakkari T, Serimaa R (1984) A study of the structure of wood cells by x-ray diffraction. Wood Sci. Technol. 18: 79–85
Preston RD (1946) The fine structure of the wall of the conifer tracheid. Proc. Roy. Soc. B133, 327–48
Preston RD (1934) Phil. Trans. B., 224, 131
Prudhomme RE, Noah J (1975) Determination of Fibril Angle Distribution in Wood Fibers: A Comparison between the X-Ray Diffraction and the Polarized Microscope Method. Wood and Fiber 6(4): 282–289
Robinson DG, Ehlers U, Herken R, Herrmann B, Mayer F, Schürmann F-W (1987) Methods of Preperation for Electron Microscopy. Springer-Verlag, Berlin, Heidelberg
Sahlberg U, Salmén L, Oscarsson A (1997) The fibrillar orientation in the S2-layer of wood fibres as determined by x-ray diffraction analysis. Wood Sci. Technol. 31: 77–86
Sell J, Zimmermann T (1997) Das Feingefüge von Holz; Spektrum der Wissenschaft, April 1997, 86–89
Wardrop AB (1952) The Low-Angle Scattering of X-Rays. Textile Research Journal April 1952, 288–291
Wardrop AB (1954) The Fine Structure of the Conifer Tracheid. Holzforschung 1: 12–29
Wardrop AB, Dadswell HE (1955) The development of the conifer tracheid, Holzforschung 2/3: 33–39
Yamamoto H, Takasi, O, Yoshida M (1993) Method of Determining the Mean Microfibril Angle of Wood over a Wide Range by the Improved Cavés Method. Mokuzai Gakkaishi 39(4): 385–381